



## Degradation of Methylene Blue by a Photo-Fenton System Based on Copper Ferrite Catalyst and Ascorbic Acid

Adika Nuzula, Indang Dewata\*, Desy Kurniawati, Jon Effendi

Chemistry Department, Faculty of Science and Education, Universitas Negeri Padang, Jl. Prof, Dr. Hamka, Padang, Indonesia

\*Corresponding Author e-mail: [indangdewata@fmipa.unp.ac.id](mailto:indangdewata@fmipa.unp.ac.id)

### Article History

Received: 09-04-2026

Revised: 18-04-2026

Published: 30-04-2026

**Keywords:** Advanced Oxidation Process; Heterogeneous Photo-Fenton; pH Optimization; Hydroxyl Radicals.

### Abstract

Water pollution caused by methylene blue is difficult to treat due to its stability and resistance to conventional methods. This study aims to evaluate the performance of a  $\text{CuFe}_2\text{O}_4$ -based photo-fenton system enhanced with ascorbic acid. The catalyst was synthesized using the sol-gel method and characterized by FTIR and XRD. Degradation experiments were carried out under UV irradiation (5 W) by varying pH (1–9) and  $\text{H}_2\text{O}_2$  concentration (1.5–15 mmol/L). Methylene blue concentration was measured using a UV-Vis spectrophotometer at a wavelength of 664 nm. The results show that degradation efficiency reached 98.48% at pH 3 and 10 mmol/L  $\text{H}_2\text{O}_2$ . This condition promotes efficient  $\text{Fe}^{2+}$  activation of  $\text{H}_2\text{O}_2$  to generate hydroxyl radicals ( $\bullet\text{OH}$ ), while ascorbic acid accelerates the reduction of  $\text{Fe}^{3+}$  to  $\text{Fe}^{2+}$ , sustaining the redox cycle and increasing radical availability. These findings demonstrate that the system is effective and has strong potential for wastewater treatment.

**How to Cite:** Nuzula, A., Dewata, I., Kurniawati, D., & Effendi, J. (2026). Degradation of Methylene Blue by a Photo-Fenton System Based on Copper Ferrite Catalyst and Ascorbic Acid. *Hydrogen: Jurnal Kependidikan Kimia*, 14(2), 380-386. <https://doi.org/10.33394/hjkk.v14i2.20202>

 <https://doi.org/10.33394/hjkk.v14i2.20202>

This is an open-access article under the [CC-BY-SA License](https://creativecommons.org/licenses/by-sa/4.0/).



## INTRODUCTION

Water pollution caused by synthetic dyes remains a serious environmental problem due to their persistence, toxicity, and resistance to conventional treatment methods (Parida et al., 2025). Among these pollutants, methylene blue is widely used in textile, paper, and pharmaceutical industries, and its discharge into aquatic systems can cause harmful effects on living organisms, including reduced light penetration and potential toxicity to aquatic life (Khan et al., 2022). Conventional treatment methods such as adsorption and biological degradation often show limited effectiveness due to the stable aromatic structure of dye molecules, as they tend to transfer pollutants from one phase to another and require long processing times, which makes them difficult to degrade completely (Lanjwani et al., 2024; Saoud et al., 2023). These limitations highlight the need for more effective treatment technologies.

Advanced oxidation processes (AOPs), particularly the photo-fenton process, have

attracted significant attention as effective methods for degrading organic pollutants. Photo-fenton process has higher efficiency in degrading color in a short period of time as well as operational flexibility, this method is considered more suitable for industrial wastewater treatment (Wijayanti et al., 2024). This process relies on the generation of highly reactive hydroxyl radicals ( $\bullet\text{OH}$ ), which can mineralize complex organic compounds into simpler and less harmful substances (Endas et al., 2026). However, conventional homogeneous Fenton systems suffer from several limitations, including narrow optimal pH conditions, sludge formation, and difficulty in catalyst recovery (Giwa et al., 2020). These drawbacks limit their practical application in large-scale wastewater treatment.

To overcome these limitations, recent studies have focused on heterogeneous catalysts such as Copper Ferrite ( $\text{CuFe}_2\text{O}_4$ ), which exhibit high chemical stability, magnetic separability, and efficient electron transfer properties. (Feng &

Zhang, 2023) reported that  $\text{CuFe}_2\text{O}_4$  can effectively activate hydrogen peroxide to produce hydroxyl radicals, leading to improved degradation of organic pollutants. However, these studies mainly emphasize catalytic activity without thoroughly addressing the limitations of the redox cycle. In particular, the slow regeneration of  $\text{Fe}^{2+}$  from  $\text{Fe}^{3+}$  has been identified as a critical factor that limits continuous hydroxyl radical production and reduces overall degradation efficiency. This limitation indicates that improving the  $\text{Fe}^{3+}/\text{Fe}^{2+}$  redox cycle is essential for enhancing the performance of heterogeneous photo-fenton systems (Li et al., 2024).

Several studies have attempted to enhance the photo-fenton system by introducing reducing agents to accelerate the  $\text{Fe}^{3+}/\text{Fe}^{2+}$  redox cycle (Noroozi et al., 2020; Zulfani & Dewajani, 2023). For instance, the addition of ascorbic acid has been reported to significantly improve catalytic performance by promoting rapid reduction of  $\text{Fe}^{3+}$  to  $\text{Fe}^{2+}$ , thereby increasing hydroxyl radical generation and improving degradation efficiency (Hou et al., 2016). Although heterogeneous photo-Fenton catalysts such as  $\text{CuFe}_2\text{O}_4$  have shown promising stability and reusability, their performance is still limited by the slow regeneration of  $\text{Fe}^{2+}$  from  $\text{Fe}^{3+}$ , which reduces continuous hydroxyl radical ( $\bullet\text{OH}$ ) production and overall degradation efficiency (Wang et al., 2017).

Based on this gap, the novelty of this study lies in the integration of a  $\text{CuFe}_2\text{O}_4$  heterogeneous catalyst with ascorbic acid as a reducing agent in a photo-fenton system, combined with a systematic evaluation of key operational parameters. This study aims to address the limitation of  $\text{Fe}^{2+}$  regeneration by enhancing the redox cycle and optimizing reaction conditions. Specifically, this research aims to synthesize and characterize  $\text{CuFe}_2\text{O}_4$  catalyst and determine the optimal conditions that maximize degradation efficiency. The results are expected to contribute to the development of more efficient and sustainable advanced oxidation systems for wastewater treatment applications.

## METHOD

### Materials and Instruments

Methylene blue (MB), copper nitrate trihydrate ( $\text{Cu}(\text{NO}_3)_2 \cdot 3\text{H}_2\text{O}$ ), iron nitrate nonahydrate ( $\text{Fe}(\text{NO}_3)_3 \cdot 9\text{H}_2\text{O}$ ), citric acid ( $\text{C}_6\text{H}_8\text{O}_7$ ), ammonia, ascorbic acid ( $\text{C}_6\text{H}_8\text{O}_6$ ),

hydrogen peroxide ( $\text{H}_2\text{O}_2$ ), sulfuric acid ( $\text{H}_2\text{SO}_4$ , 0.1 M), sodium hydroxide ( $\text{NaOH}$ , 0.1 M), and alcohol. The instruments used were UV lamps (5 W), magnetic stirrer, pH meter, centrifuge, furnace, oven, and UV-Vis spectrophotometer, FTIR and XRD are used to characterize catalysts.

### Catalyst Synthesis

$\text{CuFe}_2\text{O}_4$  nanoparticles were synthesized using the sol-gel method. Copper nitrate 0.1 mol/L, iron nitrate 0.2 mol/L, and citric acid 0.3 mol were dissolved in distilled water. Ammonia solution was added dropwise until pH 7 was reached. The mixture was heated at  $70^\circ\text{C}$  to form a gel (Soufi et al., 2022). The resulting gel was dried at  $130^\circ\text{C}$  for 7 hours and calcined at  $600^\circ\text{C}$  for 3 hours to obtain a blackish-brown powder (Feng & Zhang, 2023). The product was washed with water and alcohol, then dried to obtain the final catalyst.

### Characterization

X-ray diffraction (XRD) analysis was performed using a  $\text{Cu K}\alpha$  radiation source ( $\lambda = 0.15418 \text{ \AA}$ ) with a PANalytical X'Pert PRO instrument. The measurement was carried out over a  $2\theta$  range of  $10\text{--}90^\circ$  to identify the phase composition and estimate the crystal size (Riyanti et al., 2024). The average crystallite size of the  $\text{CuFe}_2\text{O}_4$  samples was determined from XRD data using the Scherrer equation.

$$D = \frac{K\lambda}{\beta \cos \theta}$$

In this equation,  $D$  represents the average crystallite size in nanometers. The constant  $K$  is the Scherrer factor (0.9), assuming a spherical particle shape. The parameter  $\lambda$  denotes the X-ray wavelength in nanometers,  $\beta$  is the full width at half maximum (FWHM) of the most intense diffraction peak in radians, and  $\theta$  is the Bragg diffraction angle in degrees (Oliveira et al., 2022). FTIR was used to analyze chemical structures and identify inorganic compounds in the range of  $400\text{--}4000 \text{ cm}^{-1}$  (Anceila et al., 2008). UV-Vis spectrophotometry was used to determine the absorbance of methylene blue before and after treatment (Horta et al., 2025).

### Photo-Fenton Degradation

#### Determination of Optimum pH

A 10 ppm methylene blue solution was prepared and adjusted to pH values of 1, 3, 5, 7, and 9 using 0.1 M  $\text{H}_2\text{SO}_4$  or 0.1 M  $\text{NaOH}$ . The initial absorbance ( $A_0$ ) was measured at the maximum wavelength using a UV-Vis spectrophotometer.

CuFe<sub>2</sub>O<sub>4</sub> catalyst (0.5 g/L) was added and stirred until homogeneous. Subsequently, 10 mmol/L H<sub>2</sub>O<sub>2</sub> and 1 mmol/L ascorbic acid were added. The reaction was initiated under UV irradiation (5 W) for 60 min. After irradiation, methanol was added to quench the reaction. The mixture was centrifuged and the supernatant was analyzed using UV-Vis spectrophotometry (A<sub>t</sub>). The optimum pH was determined based on the highest degradation efficiency. Degradation

efficiency (%) was calculated using the following equation :

$$\text{Degradation (\%)} = \frac{A_0 - A_t}{A_0} \times 100\%$$

#### Determination of Optimum H<sub>2</sub>O<sub>2</sub> Concentration

The experiment was repeated at the optimum pH using various H<sub>2</sub>O<sub>2</sub> concentrations. The same procedure was applied, and the optimum concentration was selected based on maximum degradation efficiency

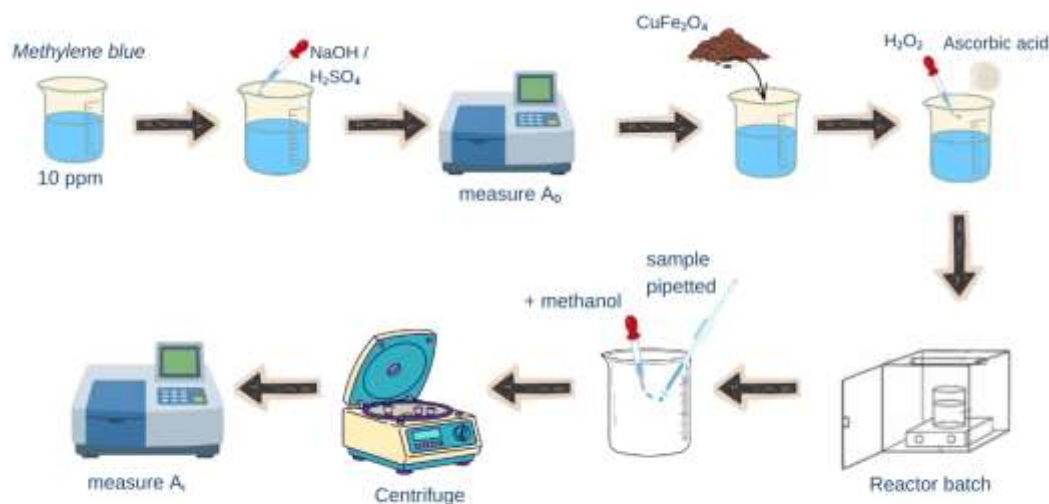


Figure 1. Work scheme for methylene blue degradation by photo-fenton method

## RESULTS AND DISCUSSION

### FTIR Characterization

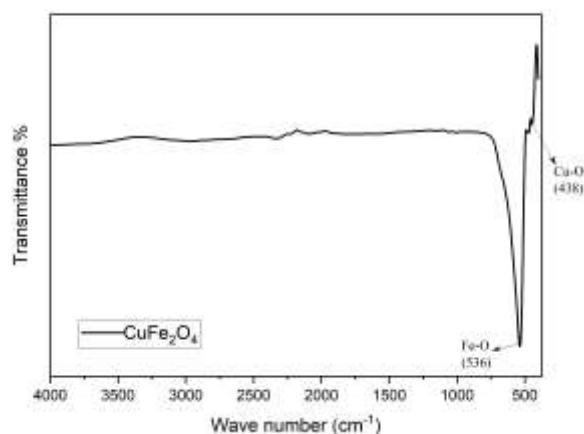


Figure 2. FTIR Spectra of CuFe<sub>2</sub>O<sub>4</sub>

FTIR analysis was performed to identify chemical bonds and confirm the formation of the synthesized material. The spectrum exhibits two main absorption bands at 536 cm<sup>-1</sup> and 438 cm<sup>-1</sup>, which correspond to characteristic metal-oxygen vibrations of spinel ferrite.

The band at 536 cm<sup>-1</sup> is assigned to the stretching vibration of Fe-O bonds, associated with Fe<sup>3+</sup> ions occupying octahedral sites. This range (500–600 cm<sup>-1</sup>) is typical for ferrite structures and confirms the formation of the iron-oxygen framework. The band at 438 cm<sup>-1</sup> is attributed to Cu-O vibrations, indicating the incorporation of Cu<sup>2+</sup> ions into tetrahedral or octahedral sites within the lattice, consistent with the typical range of 400–500 cm<sup>-1</sup> (Selima et al., 2019).

The dominance of absorption bands in the low wavenumber region, without additional peaks, indicates the absence of organic residues or precursor impurities. This suggests the formation of a relatively pure ferrite phase. The difference in band positions arises from cation distribution in the spinel structure. Fe-O bonds at octahedral sites exhibit stronger interactions, resulting in higher wavenumbers compared to Cu-O bonds (Ali et al., 2026).

The presence of Fe-O bonds indicates the availability of iron active sites that play a crucial

role in activating  $\text{H}_2\text{O}_2$  to generate hydroxyl radicals ( $\bullet\text{OH}$ ) through the Fenton reaction (Gamboa-Savoy et al., 2023), which are responsible for the degradation of organic pollutants. Meanwhile, Cu–O bonds contribute to enhanced electron transfer within the catalyst structure, facilitating the reduction of  $\text{Fe}^{3+}$  to  $\text{Fe}^{2+}$  and accelerating the  $\text{Fe}^{3+}/\text{Fe}^{2+}$  redox cycle (Sebah & Belmouden, 2025). This synergistic interaction between Fe–O and Cu–O bonds improves the continuity of hydroxyl radical production and enhances the overall catalytic performance of  $\text{CuFe}_2\text{O}_4$  in the photo-Fenton system

These results are consistent with the findings reported by (Feng & Zhang, 2023), who reported Fe–O bands at  $520\text{--}580\text{ cm}^{-1}$  and Cu–O bands at  $420\text{--}460\text{ cm}^{-1}$  for  $\text{CuFe}_2\text{O}_4$ . The consistency confirms that the synthesized material possesses the characteristic spinel structure.

### XRD Characterization

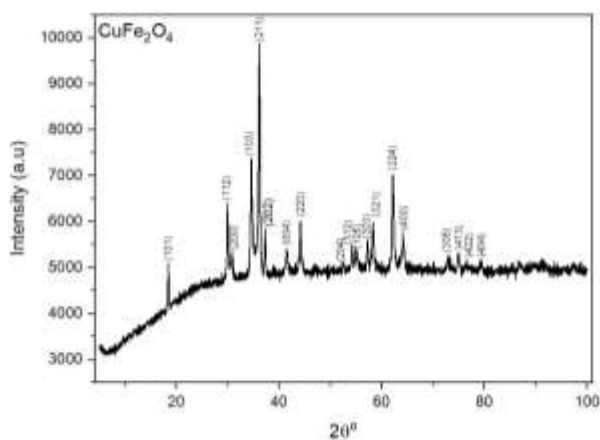


Figure 3. Diffractogram of  $\text{CuFe}_2\text{O}_4$

The XRD pattern confirms the formation of  $\text{CuFe}_2\text{O}_4$  with a spinel structure. The main diffraction peaks appear at  $2\theta = 30.81^\circ, 34.55^\circ, 36.12^\circ, 44.17^\circ, 57.19^\circ, 62.11^\circ,$  and  $64.11^\circ$ , with the highest intensity at the (211) plane. All peaks are consistent with the JCPDS standard No. 01-072-1174, indicating the formation of a pure  $\text{CuFe}_2\text{O}_4$  phase without detectable impurities. This result demonstrates that the synthesis method effectively controlled phase formation.

The crystallite size, calculated using the Scherrer equation is 42.9 nm. These results are consistent with previous studies reporting  $\text{CuFe}_2\text{O}_4$  crystallite sizes in the range of 20–60 nm with similar diffraction patterns (Yadav et al., 2017). The obtained crystallite size of  $\text{CuFe}_2\text{O}_4$  indicates that the material is in the nanocrystalline scale, which has a significant impact on catalytic

activity. Smaller crystallite size results in a higher surface area to volume ratio (Eker et al., 2024). This means that more atoms are located on the surface rather than in the bulk structure, thereby increasing the number of active sites available for the reaction (Joudeh & Linke, 2022).

A relatively small crystallite size allows more Fe ions to be exposed on the surface, increasing the number of active sites that can interact with  $\text{H}_2\text{O}_2$ . As a result, the generation of hydroxyl radicals ( $\bullet\text{OH}$ ) becomes more efficient because more  $\text{Fe}^{2+}$  is available to activate  $\text{H}_2\text{O}_2$  (Gallo-Cordova et al., 2025). Furthermore, a larger surface area increases the contact between the catalyst and methylene blue molecules, thereby accelerating the adsorption and oxidation processes (Liu et al., 2019).

### Effect of pH on Methylene Blue Degradation

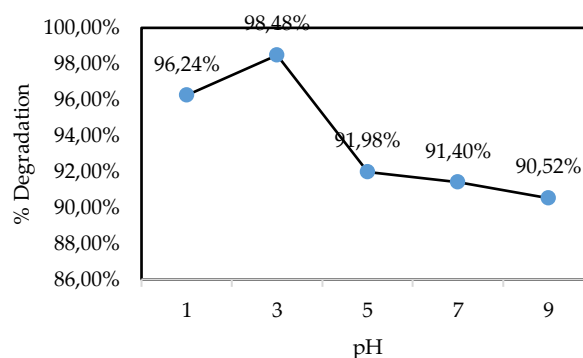


Figure 4. Degradation pH variation

The results show that pH strongly affects methylene blue degradation efficiency. Based on the data efficiency increased from 96.24% at pH 1 to a maximum of 98.48% at pH 3, then decreased to 91.98%, 91.40%, and 90.52% at pH 5, 7, and 9, respectively. This trend indicates that pH 3 is the optimum condition for the photo-Fenton process.

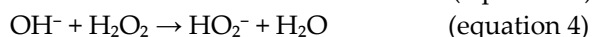
Highly acidic conditions increase the solubility of catalytic metal ions, allowing the formation of hydroxyl radicals ( $\bullet\text{OH}$ ) to proceed optimally. At pH 1, excessively low pH leads to an excess of  $\text{H}^+$  ions can interact with  $\text{H}_2\text{O}_2$  to form a protonated species,  $\text{H}_3\text{O}_2^+$  (equation 2) which has lower reactivity compared to free  $\text{H}_2\text{O}_2$ .  $\text{H}_3\text{O}_2^+$  can act as a scavenger of  $\bullet\text{OH}$  radicals (Rusevova Crincoli & Huling, 2020), thereby reducing the number of radicals available to effectively oxidize methylene blue.

At pH 3,  $\text{Fe}^{2+}/\text{Fe}^{3+}$  remain soluble and active, enabling maximum generation of hydroxyl radicals ( $\bullet\text{OH}$ ) through the Fenton reaction, which drives efficient dye oxidation (equation 1).

The results are consistent with previous studies (Giwa et al., 2020) and support the hypothesis that pH controls the efficiency of the photo-Fenton degradation process.



At higher pH (> 4), efficiency decreases due to  $\text{Fe}^{3+}$  hydrolysis and formation of  $\text{Fe}(\text{OH})_3$  precipitates, which reduce active catalyst availability. In neutral to alkaline conditions (pH 7–9), the effect becomes more pronounced due to dominant iron precipitation and non-productive decomposition of  $\text{H}_2\text{O}_2$  into  $\text{H}_2\text{O}$  and  $\text{O}_2$  (equation 3). Additionally,  $\bullet\text{OH}$  radicals become unstable and transform into less reactive species ( $\text{HO}_2^-$ ) (equation 4), further limiting oxidation (Endas et al., 2025).



### Effect of $\text{H}_2\text{O}_2$ Concentration on Methylene Blue Degradation

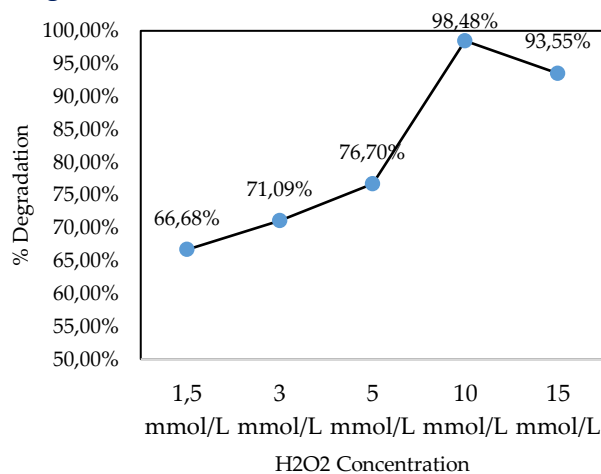


**Figure 5. Degradation of  $\text{H}_2\text{O}_2$  Concentration Variation**

The results show that increasing  $\text{H}_2\text{O}_2$  concentration from 1.5 to 10 mmol/L enhances methylene blue degradation efficiency from 66.68% to 98.48%, indicating that  $\text{H}_2\text{O}_2$  effectively promotes the formation of hydroxyl radicals ( $\bullet\text{OH}$ ) through the Fenton reaction with  $\text{Fe}^{2+}$  (equation 1). These radicals act as the main oxidizing species that rapidly degrade the dye structure, explaining the positive trend observed at lower concentrations, consistent with Sugeng et al., 2020.

However, at 15 mmol/L, the efficiency decreases to 93.55% due to the scavenging effect, where excess  $\text{H}_2\text{O}_2$  reacts with  $\bullet\text{OH}$  to form less

reactive hydroperoxyl radicals ( $\text{HO}_2\bullet$ ) (equation 5), thereby reducing the availability of active radicals for degradation. This behavior aligns with (Endas et al., 2025), confirming that excessive oxidant inhibits the reaction.



## CONCLUSION

This study demonstrates that the  $\text{CuFe}_2\text{O}_4$ -based photo-fenton system enhanced with ascorbic acid effectively degrades methylene blue due hydroxyl radical ( $\bullet\text{OH}$ ) generation under optimal conditions (pH 3 and 10 mmol/L  $\text{H}_2\text{O}_2$  concentration). However, the study is limited to controlled laboratory conditions using model solutions, which do not fully represent the complexity of real wastewater, and the requirement of acidic pH, UV irradiation, and chemical inputs poses challenges for large-scale application in terms of cost, energy, and operational feasibility. Although the system shows high efficiency, its direct implementation in real-world treatment remains constrained by issues such as catalyst stability, recovery, and potential iron leaching. Therefore, future research should focus on testing in real wastewater, improving catalyst reusability, optimizing operation under milder conditions, and reducing energy and chemical consumption to enhance the practicality and scalability of the process.

## RECOMMENDATION

Future studies should further investigate strategies to mitigate iron precipitation under neutral to alkaline pH conditions, explore alternative reducing agents, and compare the performance of  $\text{CuFe}_2\text{O}_4$  with other catalysts under similar conditions to improve system efficiency. In addition, further evaluation using real wastewater samples is necessary to assess the practical applicability of the system.

## BIBLIOGRAPHY

- Ali, S., Hemed, O. M., Elhussiny, F., Mahgoub, M. H., Mohammed, S., & Elmekawy, A. (2026). Structural, optical, and magnetic characterization of Cu-Zn-Ni spinel ferrite nanoparticles with antibacterial potential. *Scientific Reports*, 16(1), 3053. <https://doi.org/10.1038/s41598-025-34792-9>
- Anceila, D., Nirmala, G. F., Sagayaraj, P., & Joseph, V. (2008). Study on optical, magnetic and structural Properties of  $\text{CuFe}_2\text{O}_4$  by Co-precipitation technique. *International Research Journal of Engineering and Technology*, 9001. [www.irjet.net](http://www.irjet.net)

- Eker, F., Duman, H., Akdaşçı, E., Bolat, E., Sarıtaş, S., Karav, S., & Witkowska, A. M. (2024). A Comprehensive Review of Nanoparticles: From Classification to Application and Toxicity. In *Molecules* (Vol. 29, Number 15). Multidisciplinary Digital Publishing Institute (MDPI). <https://doi.org/10.3390/molecules29153482>
- Endas, L., Akpah, B. C., Anaegbu, J., & Kure, A. (2026). Unveiling the effectiveness of the photo-Fenton process for the mineralization of textile dyes: A kinetic and thermodynamic study. *Science World Journal*, 20(4), 1752–1758. <https://doi.org/10.4314/swj.v20i4.58>
- Endas, L., Kure, A., & Anaegbu, J. O. (2025). Optimization of Photo-Fenton process for the degradation of basic red 9: Kinetic analysis, intermediate identification, and toxicity implications. *Science World Journal*, 20(4), 1759–1765. <https://doi.org/10.4314/swj.v20i4.59>
- Feng, J., & Zhang, Y. (2023). Ascorbic acid enhanced CuFe<sub>2</sub>O<sub>4</sub>-catalyzed heterogeneous photo-Fenton-like degradation of phenol. *Journal of Environmental Chemical Engineering*, 11(5). <https://doi.org/https://doi.org/10.1016/j.jece.2023.111009>
- Gallo-Cordova, A., Nuñez, N., Díaz-Ufano, C., Veintemillas-Verdaguer, S., Soler-Morala, J., Palomares, F. J., Lima, E., Winkler, E. L., & Morales, M. del P. (2025). Insights into the formation of free radicals using metal ferrite nanocatalysts (MFe<sub>2</sub>O<sub>4</sub>, M = Fe, Mn, Zn, Co) prepared by a highly reproducible microwave-assisted polyol method. *Nanoscale*, 17(33), 19182–19195. <https://doi.org/10.1039/d5nr02101d>
- Gamboa-Savoy, F., Onfray, C., Hassan, N., Salazar, C., & Thiam, A. (2023). Enhanced catalytic reduction of emerging contaminant by using magnetic CuFe<sub>2</sub>O<sub>4</sub>@MIL-100(Fe) in Fenton-based electrochemical processes. *Chemosphere*, 337. <https://doi.org/10.1016/j.chemosphere.2023.139231>
- Giwa, A. R. A., Bello, I. A., Olabintan, A. B., Bello, O. S., & Saleh, T. A. (2020). Kinetic and thermodynamic studies of fenton oxidative decolorization of methylene blue. *Heliyon*, 6(8). <https://doi.org/10.1016/j.heliyon.2020.e04454>
- Horta, I., Neto, N. F. A., Kito, L. T., Miranda, F., Thim, G., Pereira, A. L. de J., & Pessoa, R. (2025). Ultra-Trace Monitoring of Methylene Blue Degradation via AgNW-Based SERS: Toward Sustainable Advanced Oxidation Water Treatment. *Sustainability (Switzerland)*, 17(10). <https://doi.org/10.3390/su17104448>
- Hou, X., Huang, X., Ai, Z., Zhao, J., & Zhang, L. (2016). Ascorbic acid/Fe@Fe<sub>2</sub>O<sub>3</sub>: A highly efficient combined Fenton reagent to remove organic contaminants. *Journal of Hazardous Materials*, 310, 170178. <https://doi.org/https://doi.org/10.1016/j.jhazmat.2016.01.020>
- Joudeh, N., & Linke, D. (2022). Nanoparticle classification, physicochemical properties, characterization, and applications: a comprehensive review for biologists. In *Journal of Nanobiotechnology* (Vol. 20, Number 1). BioMed Central Ltd. <https://doi.org/10.1186/s12951-022-01477-8>
- Khan, I., Saeed, K., Zekker, I., Zhang, B., Hendi, A. H., Ahmad, A., Ahmad, S., Zada, N., Ahmad, H., Shah, L. A., Shah, T., & Khan, I. (2022). Review on Methylene Blue: Its Properties, Uses, Toxicity and Photodegradation. In *Water (Switzerland)* (Vol. 14, Number 2). MDPI. <https://doi.org/10.3390/w14020242>
- Lanjwani, M. F., Tuzen, M., Khuhawar, M. Y., & Saleh, T. A. (2024). Trends in photocatalytic degradation of organic dye pollutants using nanoparticles: A review. *Inorganic Chemistry Communications*, 159, 111613. <https://doi.org/10.1016/j.inoche.2023.111613>
- Li, L., Guo, J., Zheng, K., Heng, H., Zhang, Y., Xie, C., Yin, M., & Zhou, B. (2024). MoS<sub>2</sub>-mediated active hydrogen modulation to boost Fe<sup>2+</sup> regeneration in solar-driven electro-Fenton process. *Journal of Hazardous Materials*, 470. <https://doi.org/10.1016/j.jhazmat.2024.134274>
- Liu, J., Du, Y., Sun, W., Chang, Q., & Peng, C. (2019). Preparation of new adsorbent-supported Fe/Ni particles for the removal of crystal violet and methylene blue by a heterogeneous Fenton-like reaction. *RSC Advances*, 9(39), 22513–22522. <https://doi.org/10.1039/c9ra04710g>
- Noroozi, R., Gholami, M., Farzadkia, M., & Jafari, A. J. (2020). Catalytic potential of CuFe<sub>2</sub>O<sub>4</sub>/GO for activation of peroxymonosulfate in metronidazole degradation: study of mechanisms. <https://doi.org/10.1007/s40201-020-00518-4/Published>
- Oliveira, T. P., Rodrigues, S. F., Marques, G. N., Costa, R. C. V., Lopes, C. G. G., Aranas, C., Rojas, A., Rangel, J. H. G., & Oliveira, M. M. (2022). Synthesis, Characterization, and Photocatalytic Investigation of CuFe<sub>2</sub>O<sub>4</sub> for the Degradation of Dyes under Visible Light. *Catalysts*, 12(6). <https://doi.org/10.3390/catal12060623>
- Parida, V. K., Singh, N., Priyadarshini, M., Kumari, P., Datta, D., & Tambi, A. (2025). Insights into the synthetic dye contamination in textile wastewater: Impacts on aquatic ecosystems and human health, and eco-friendly remediation strategies for environmental sustainability. In *Journal of Industrial and Engineering Chemistry* (Vol. 150, pp. 247–264). Korean Society of Industrial Engineering Chemistry. <https://doi.org/10.1016/j.jiec.2025.04.019>
- Riyanti, F., Hariani, P. L., Hasanudin, H., Rachmat, A., & Purwaningrum, W. (2024). Optimization Photodegradation of Methylene Blue Dye using Bentonite/PDA/Fe<sub>3</sub>O<sub>4</sub>@CuO Composite by

- Response Surface Methodology. *Bulletin of Chemical Reaction Engineering and Catalysis*, 19(2), 252–264. <https://doi.org/10.9767/bcrec.20132>
- Rusevova Crincoli, K., & Huling, S. G. (2020). Hydroxyl radical scavenging by solid mineral surfaces in oxidative treatment systems: Rate constants and implications. *Water Research*, 169. <https://doi.org/10.1016/j.watres.2019.115240>
- Saoud, T., Benramache, S., & Diha, A. (2023). The Effect of Co and Cu CO-Doping ZnO Thin Film On Structural and Optical Properties. *Chemistry, Didactics, Ecology, Metrology*, 28(1–2), 171–178. <https://doi.org/10.2478/cdem-2023-0010>
- Sebah, I., & Belmouden, M. (2025). Copper ferrite-graphene oxide catalyst for enhanced peroxymonosulfate activation and pollutant degradation. *Nanoscale Advances*, 7(18), 5646–5657. <https://doi.org/10.1039/d5na00409h>
- Selima, S. S., Khairy, M., & Mousa, M. A. (2019). Comparative studies on the impact of synthesis methods on structural, optical, magnetic and catalytic properties of CuFe<sub>2</sub>O<sub>4</sub>. *Ceramics International*, 45(5), 6535–6540. <https://doi.org/10.1016/j.ceramint.2018.12.146>
- Soufi, A., Hajjaoui, H., Elmoubarki, R., Abdennouri, M., Qourzal, S., & Barka, N. (2022). Heterogeneous Fenton-like degradation of tartrazine using CuFe<sub>2</sub>O<sub>4</sub> nanoparticles synthesized by sol-gel combustion. *Applied Surface Science Advances*, 9. <https://doi.org/10.1016/j.apsadv.2022.100251>
- Sugeng, E. J., de Cock, M., Leonards, P. E. G., & van de Bor, M. (2020). Toddler behavior, the home environment, and flame retardant exposure. *Chemosphere*, 252. <https://doi.org/10.1016/j.chemosphere.2020.126588>
- Wang, P., Zhou, X., Zhang, Y., Yang, L., Zhi, K., Wang, L., Zhang, L., & Guo, X. (2017). Unveiling the mechanism of electron transfer facilitated regeneration of active Fe<sup>2+</sup> by nano-dispersed iron/graphene catalyst for phenol removal. *RSC Advances*, 7(43), 26983–26991. <https://doi.org/10.1039/c7ra04312k>
- Wijayanti, K. A., Hakika, D. C., Setyawan, M., Suhendra, Amal, I., & Biddinika, M. K. (2024). Recalcitrant Industrial Wastewater Treatment Using Fenton and Photo-Fenton Oxidation: A Comparison Study. *Indonesian Journal of Environmental Management and Sustainability*, 8(3), 100–109. <https://doi.org/10.26554/ijems.2024.8.3.100-109>
- Yadav, R. S., Kuritka, I., Vilcakova, J., & Havlica, J. (2017). Structural, dielectric, electrical and magnetic properties of CuFe<sub>2</sub>O<sub>4</sub> nanoparticles synthesized by honey mediated sol-gel combustion method and annealing effect. *Journal of Materials Science: Materials in Electronics*, 28(8). <https://doi.org/10.1007/s10854-016-6305-4>
- Zulfani, M. R., & Dewajani, H. (2023). Pengaruh Penambahan Chelating Agents (Asam Askorbat, Hidroksilamina, dan Asam Oksalat) dalam Fenton-Like Reaction pada Proses Degradasi Metilen Biru. *DISTILAT: Jurnal Teknologi Separasi*, 9(3), 286–294. <https://doi.org/10.33795/distilat.v9i3.3759>